

A RECIRCULATING LINAC AS A CANDIDATE FOR THE UK NEW LIGHT SOURCE

P.H. Williams*, D. Angal-Kalinin, S.L. Smith,
ASTeC, STFC Daresbury Laboratory & Cockcroft Institute, UK
R. Bartolini, I.P. Martin, Diamond Light Source Ltd. & John Adams Institute, UK

Abstract

We describe a design for a two-pass recirculating 1.3 GHz superconducting linac as a driver for the suite of free-electron lasers proposed in the UK New Light Source project. The machine will deliver longitudinally compressed electron bunches with repetition rates of 1 kHz with an initial upgrade path to increase this to 1 MHz. A modular philosophy is employed to separate beam injection and extraction from a three stage compression scheme. Results show that the necessary high peak currents can be achieved whilst preserving beam quality.

INTRODUCTION

The New Light Source project [1] was launched in April 2008 by the UK Science and Technology Facilities Council (STFC) to consider the scientific case and develop a conceptual design for a possible next generation light source. The facility will be based on a combination of advanced conventional laser and free-electron laser (FEL) sources.

The NLS accelerator design specifications are to produce electron bunches with ~ 1 mm mrad transverse slice emittance, peak current above 1 kA and slice energy spread less than 5×10^{-4} . Initially, the facility will utilise a normal conducting L-Band photoinjector [2] to deliver bunch repetition rates of up to 1 kHz to three seeded FELs covering photon energies from 50 eV to 1 keV [3, 4]. An upgrade will see a high repetition rate gun delivering bunch rates up to 1 MHz, currently a VHF design is being explored [5].

Two designs are currently being evaluated for the NLS accelerator; a single pass machine consisting of fourteen TESLA type cryomodules [6]; and a two pass recirculating machine consisting of nine TESLA type cryomodules. The latter is described in this paper.

Accelerator components succeeding the linac are common to both designs and consist of a beam switchyard, collimation and diagnostic tomography section, these are described in a separate paper [7].

Motivations for considering a recirculating machine in comparison to a single pass machine include: reduced capital and running costs; shorter footprint; ease of extraction of multiple energy beams; and a natural upgrade path to higher energy. Issues in comparison to a single pass machine include: additional injection and extraction sections; restrictions to the bunch compression scheme; synchrotron

radiation effects in translating sections; and more stringent jitter tolerances.

COMPONENTS & OPTICS

Figure 1 shows the optics functions for the proposed machine. The design philosophy is to minimise any bunch compression from components not dedicated for that purpose, in other words separating as much as possible transverse and longitudinal manipulations. In this way, one retains the ability to tailor the final bunch profile in a flexible way.

In the current configuration we set the field gradient of the 1.3 GHz cavities to 17.5 MV/m.

Injection at 200 MeV

The gun is followed by two cryomodules, the first of whose cavities are fed from individual power supplies to enable independent phase and voltage control for emittance compensation in the gun.

Tracking using the code Elegant [8] commences at this location. The beam is decelerated and linearised in longitudinal phase space using a third harmonic (3.9 GHz) system capable of achieving 15 MV/m in CW operating mode. The particular gradient required to linearise the bunch is a function not only of the accelerating RF, but also of the T_{566} and U_{5666} in subsequent components such as the injection merge and arcs. These components have been designed in order to minimise the third harmonic gradient required. Microbunching is then smeared by increasing the incoherent energy spread of the bunch using a laser heater [9]. This is followed by the first four-dipole C-type compressor chicane, which reduces the bunch length from 20 ps to 5 ps FW.

Now at an energy of 200 MeV, the beam enters an isochronous and achromatic injection dogleg section. This uses two dipoles in addition to the last dipole of a standard four dipole chicane, which is that traversed by the high energy beam. Because of the $\mathcal{O}(3\%)$ energy spread required for later compression, it is important that the dogleg is well behaved at second order in the transfer matrices. To achieve this, a system of eight quadrupoles and three sextupoles is employed (together with four preceding matching quadrupoles). A layout with low natural chromaticities and second order dispersion (T_{166}) is established prior to the sextupole insertion. The sextupoles are then optimised to set T_{166} to zero, this further suppresses the chromatic

*peter.williams@stfc.ac.uk

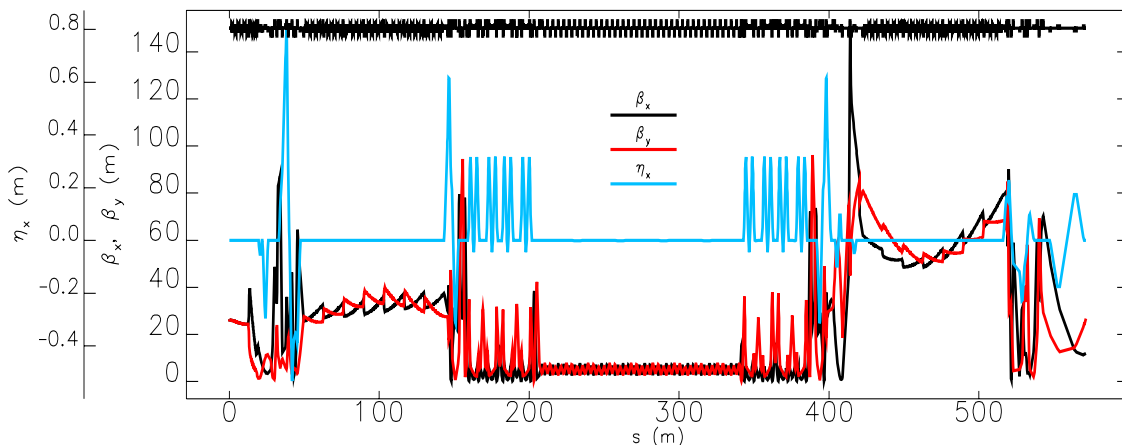


Figure 1: Optics functions from second injector cryomodule to final compressor at the end of the second linac pass.

terms as detailed in [10]. An unwanted consequence of this approach is that we are left with a small, but significant longitudinal curvature, $T_{566} = -0.35$, which necessitates an increased gradient in the third harmonic cavity to that which would be required otherwise. Figure 2 shows

able limits.

Linac First Pass & Extraction at 1.2 GeV

On first pass through the seven cryomodules of the main linac, the beam energy is raised to 1.2 GeV. To extract and separate the 1.2 GeV and 2.2 GeV beams, an achromatic dogleg is employed which also matches the 1.2 GeV beam to the arc. The extraction dipole bends the 1.2 GeV beam 10° , five quadrupoles and one sextupole within the dogleg are followed by a -10° dipole and four quadrupoles which match to the arc. The system has an $R_{56} = 7$ mm. As with the injection, it is paramount to minimise second order effects and an analogous process was followed to ensure this. Figure 3 shows the optics functions, emittances and layout for the extraction.

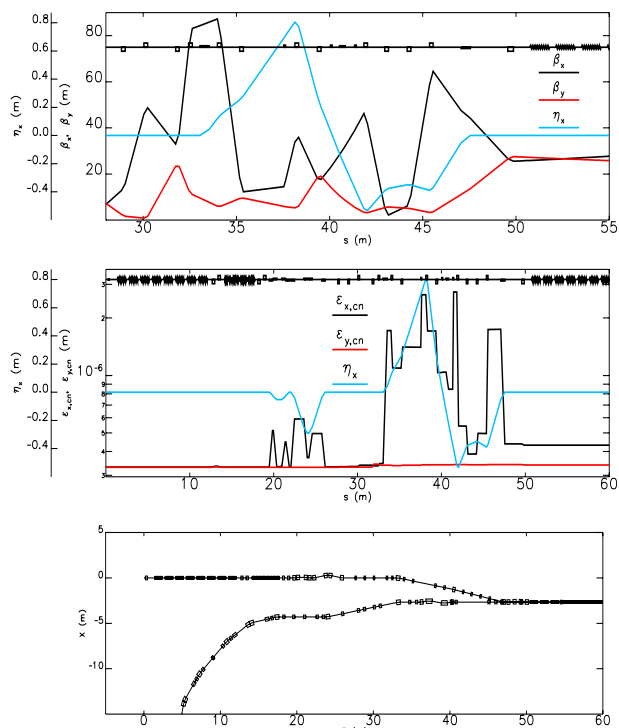


Figure 2: Optics functions, tracked projected normalised emittances and layout of injector.

the optics functions, emittances (less dispersive contributions) and layout. It is seen that there is horizontal emittance increase from 0.3 to 0.48 mm mrad (spikes in dispersive regions are spurious and arise from the non-gaussian nature of the tracked bunches). This is due to chromatic effects rather than synchrotron radiation emission and although further work will aim to reduce this, is within toler-

Arcs

A number of candidate arc lattices were studied before alighting on one based on the BESSY-FEL design [11]. Each 180° arc consists of four triple-bend achromats ($\pi/12$ dipole bend angle) and was chosen due to the small ISR induced emittance dilution of the beam (4% total for both arcs). CSR does not degrade the beam significantly if the bunch length is kept above 2 ps FW through the arcs. The ISR induced incoherent energy spread of $\sim 5 \times 10^{-5}$ is actually fortuitous as it enables the laser power within the laser heater to be reduced whilst still suppressing microbunching. On traversal of the non-isochronous arcs the bunch length is reduced from 5 ps to 3 ps FW. There is relative freedom to tune the T_{566} in the arcs allowing reduction of the linearising voltage in the third harmonic system. The return transport connecting the two arcs contains a system to independently adjust the path length between the two arcs over one RF wavelength. This consists of a focused movable girder dogleg pair [12] and allows the RF phase seen on the second linac pass to be varied independently to that of the first pass.

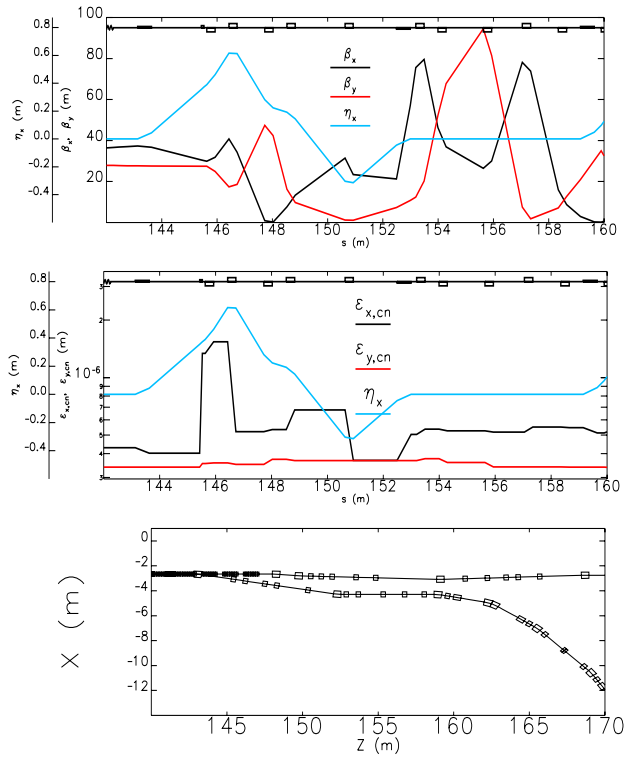


Figure 3: Optics functions, tracked projected normalised emittances and layout of extraction.

Re-injection at 1.2 GeV & Linac Second Pass

Exiting the second arc, the beam enters the exact reverse of the 1.2 GeV extraction system. This is followed by the second four-dipole compressor chicane, which is of S-type in order to reduce emittance growth due to coherent synchrotron radiation (CSR) emission. The horizontal beta function is minimised in the fourth dipole, again to suppress CSR. It then traverses the high-energy branch of the injection system, giving a small $R_{56} = 4$ mm. On arrival at the linac for the second pass, the bunch length has thus been reduced from 3 ps to 800 fs. Figure 4 shows the optics functions and emittances for the re-injection system. We see that there is significant horizontal emittance growth from 0.53 to 0.88 mm mrad, this predominantly originates in chromatic contributions in the reverse of the 1.2 GeV extraction. It is therefore likely that this component will subsequently be replaced, possibly by merely increasing the radius of the second arc with respect to the first. There is also an increase from 0.88 to 1.04 mm mrad in the shallow C-type linac injection chicane, this originates from CSR.

The beam then passes through the linac for the second time, this time on crest and emerges at 2.2 GeV.

Extraction at 2.2 GeV & Final Compression

The high-energy branch of the extraction system is achromatic and has an $R_{56} = 0.04$ mm. It consists of three dipoles in addition to the extraction dipole and ten

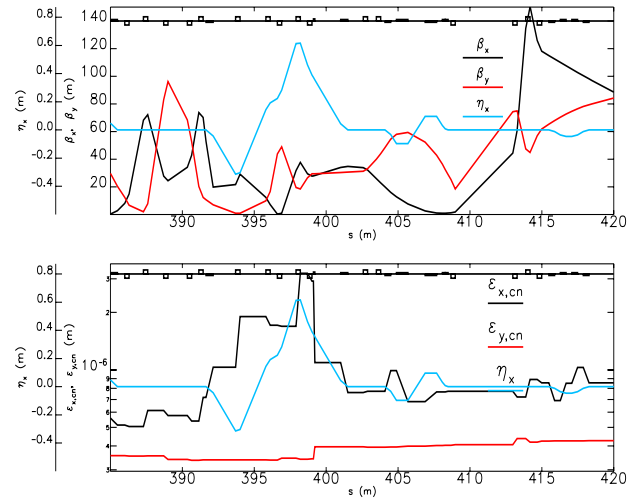


Figure 4: Optics functions and tracked projected normalised emittances at re-injection.

quadrupoles. In analogy to the 1.2 GeV extraction the second order terms are minimised, however in this case no sextupole correction is necessary. The final four-dipole compression chicane is of S-type to minimise CSR emittance growth. Here the bunch achieves a final length of 300 fs FW.

START TO END SIMULATIONS

Collective effects included in the simulations are longitudinal space charge, ISR and CSR as implemented in the one dimensional approximation, as well as linac wakefields. Table 1 shows the machine parameters selected to produce

Position	Variable	Value	Unit
3.9 GHz Lineariser	V	15	MV/m
Lineariser	ϕ	+162.1	$^\circ$
Laser Heater	Spot Size	0.7	mm
Laser Heater	Power	5.0	MW
1.3 GHz Modules	V	17.5	MV/m
Injector	ϕ	-25.1	$^\circ$
Linac first pass	ϕ	-10.0	$^\circ$
Linac second pass	ϕ	0.0	$^\circ$
First compressor	R_{56}	97.2	mm
Arcs (full 360 $^\circ$)	R_{56}	37.3	mm
Second compressor	R_{56}	72.8	mm
Third compressor	R_{56}	26.3	mm

Table 1: Machine parameters relevant to production of longitudinal phase space at 200 pC. Phases are with respect to crest.

the final bunch as presented. It is proposed to further develop this working point using a Nelder-Mead simplex optimiser taking into account the specifics of the proposed HHG seeding scheme proposed for the NLS FELs. We see

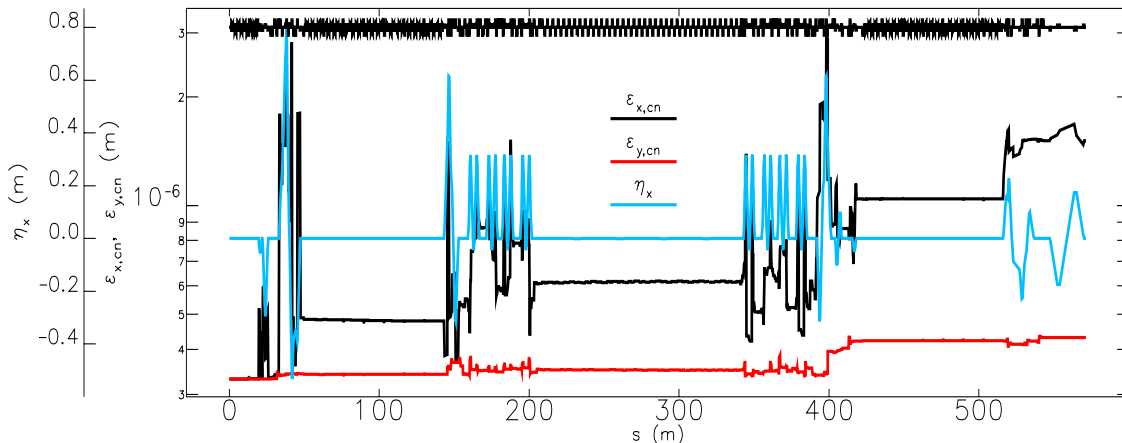


Figure 5: Projected normalised emittances (and horizontal dispersion) through machine.

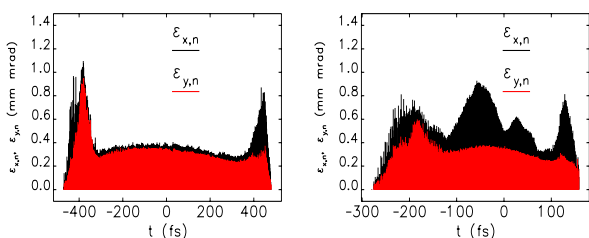


Figure 6: Normalised slice emittances before (left) and after (right) final compression.

from Fig. 6 that we are able to preserve near gun-like slice emittances right up until final compression, after having traversed all injection and extraction components. Even after final compression slice emittances remain below 1 mm mrad along the entire bunch. One should bear in mind however, that the beam switchyard will further degrade this. The remaining final bunch properties are shown in Fig. 7.

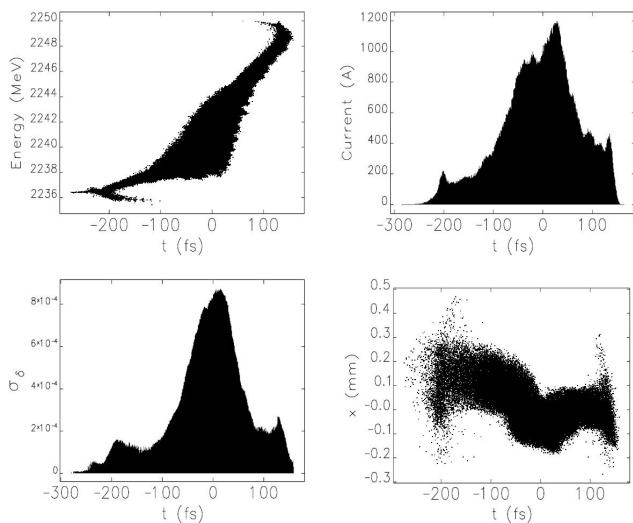


Figure 7: Final bunch properties: (1) longitudinal phase space, (2) current profile, (3) slice energy spread & (4) horizontal-transverse distribution.

We see that we are able to satisfy the required bunch parameters demanded with the exception of the slice energy spread. This is a sensitive function of the laser heater power and will require further study of microbunching effects in order to minimise.

CONCLUSIONS

It is shown in [4] that bunches from this recirculator are capable of driving an FEL. The results presented here are a significant improvement on those earlier simulations. A recirculating linac is therefore a promising candidate to drive a suite of seeded FELs such as that envisaged for the NLS project.

ACKNOWLEDGEMENTS

The authors wish to thank Dave Douglas, Geoff Krafft and Richard Walker for useful discussions.

REFERENCES

- [1] J. Marangos *et al.*, NLS Science Case & Outline Design Report, <http://www.newlightsource.org>.
- [2] J.-H. Han, TUPC44, these proceedings.
- [3] N. R. Thompson *et al.*, WEO02, these proceedings.
- [4] D. Dunning *et al.*, MOPC69, these proceedings.
- [5] J. W. McKenzie, *et al.*, TUPC41, these proceedings.
- [6] R. Bartolini *et al.*, WEOB02, these proceedings.
- [7] D. Angal-Kalinin *et al.*, WEPC17, these proceedings.
- [8] M. Borland, Advanced Photon Source, LS-287 (2000).
- [9] Z. Huang *et al.*, Phys. Rev. ST Accel. Beams **7**, 074401 (2004).
- [10] R. J. England *et al.*, Phys. Rev. ST Accel. Beams **8**, 012801 (2005).
- [11] M. Abo-Bakr *et al.*, BESSY-FEL Technical Design Report, 2004.
- [12] P. H. Williams & H. L. Owen, 4GLS Design Report 14, Daresbury Laboratory, 2006.